10A.1 Urban Flood Monitoring using X-band Dual-polarization Radar Network: Program of the CASA-NIED partnership

V. Chandrasekar[(1)*], Y. Wang[(1)], M. Maki[(2)], and T. Maesaka[(2)]

[(1)] Colorado State University
1373 Campus Delivery
Fort Collins, CO 80523, USA

[(2)] National Research Institute for Earth Science and Disaster Prevention
Tsukuba, Japan

1. INTRODUCTION

Flooding is one of the most common natural hazards in the world. Every year, according to a National Academy report, floods are responsible for more deaths nationwide than any other weather phenomenon, with a 30-year average of more than 120 fatalities per year (NRC 2005). Especially, heavy development decreases the response time of urban watersheds to rainfall and increases the chance of localized flooding events over a small spatial domain. Successful monitoring of urban floods requires high spatiotemporal resolution, accurate precipitation estimation because of the rapid flood response as well as the complex hydrologic and hydraulic characteristics in an urban environment.

Radar observation of high temporal and spatial resolutions has shown great potential to drive flood forecasting by incorporating distributed hydrological models (Vieux and Bedient 2004). Modern Distributed Collaborative Adaptive Sensing (DCAS) radar network is capable of high-resolution observation over a large coverage area (Chandrasekar et al. 2008). The network centric sensing paradigm greatly improves the system capability and measurement accuracy (Junyent and Chandrasekar 2008). By reducing the maximum range and operating at X-band, one can ensure good cross range resolution with a small-size antenna and keep the radar beam closer to the ground. The sensing node can be constructed from small-size radar units that are easily amenable to ubiquitous urban deployment. A recent National Academy study has explained the virtues of the DCAS system for complex terrain (NRC 2008).

The Center for Collaborative Adaptive Sensing of the Atmosphere (CASA) is developing the technologies and the systems for network centric weather observation. A four-node X-band dual-polarization radar network has been in operation in Oklahoma, which is referred as the IP1 (Integrative Project 1). In Japan, the National Research Institute for Earth Science and Disaster Prevention (NIED) is establishing an X-band dual-polarization radar network (X-NET) in Metropolitan Tokyo area. CASA and NIED have formed a partnership to initiate a joint program for urban flood monitoring using X-band dual-polarization radar network. Polarimetric radar based technologies are implemented for real-time mitigation of rain attenuation and accurate estimation of rainfall. This paper reviews various aspects in radar rainfall mapping in urban coverage using X-band dual-polarization radar networks. This paper will also present the preliminary plan for the joint program of CASA-NIED partnership.

2. RADAR RAINFALL MAPPING USING DENSE RADAR NETWORK

Radar quantitative precipitation estimation (QPE) is one of the key products that will drive the hydrologic models for floods monitoring. High resolution rainfall mapping over a large area is the fundamental strength of weather radar in this kind of applications. In urban environment, the replacement of vegetation by impermeable surface and the construction of drainage networks reduce the response time of urban watersheds to rainfall but also increase the peak discharge volumes. Road, channels, buildings and other structures modify the hydrologic and hydraulic characteristics and potentially increase the chance of localized flooding events. Predication of lumped discharge from the target basin is not sufficient in this case for efficient floods warning and prevention.

* *Corresponding author address:* V. Chandrasekar, Colorado State University, Fort Collins, CO 80523-1373; email: chandra@engr.colostate.edu.

The accuracy of radar QPE relies both on the radar system, such as beamwidth and sidelobe, and on the environmental factors, such as clutter and storm variability. Radar beam can overshoot the lower part of atmosphere due to blockages of the earth's curvature or local terrain. Radar observations can also be contaminated by hail, melting hydrometeor particles, and/or ground clutter. In addition, in urban environment, strong clutter is expected due to scattering from buildings in the neighborhood which act as perfect reflectors when radar is steered down low.

2.1. Spatial Resolution

For urban floods monitoring, high resolution hydrologic model has been developed on the order of tens of meters (Maki et al 2008). To realize its full capability needs rainfall estimates of commensurate resolution. Additionally, beam broadening can also affect the quality of polarimetric radar measurements in the presence of non-uniform beam filling (Ryzhkov 2007). At long radar ranges, the radar beam extends a wider distance across beam such that large gradients are more likely presented, which can result in substantial biases. One of the motivations of a networked sensing system is to achieve good cross-beam resolution using small range radars. In the current operational national network NEXRAD, each radar node probes the storm up to 460 km, or 300 km in super-resolution mode, with 1^o beam. This corresponds to a cross-beam distance larger than 5 km, virtually preventing reliable quantitative rainfall estimates because of storm gradients either in vertical or in horizontal direction. NEXRAD delivers QPE products in 4X4 km grids. If the range is contained within 40 km, the cross-beam distance will be scaled down to 700 meters and QPE products can be generated in much smaller grids.

2.2. Temporal Resolution

High temporal resolution is required in order to track such quick response and predict the threats in the same time scale using real-time radar rainfall. The current NEXRAD observations are updated in every 5~6 minutes. Because radar measures the instantaneous rainfall rate, coarse temporal update rate likely leaves substantial sampling gaps in radar QPE for the cases of fast moving storms. Small sampling interval will be particularly valuable in the extreme rain storms. It only takes 30~60 minutes for an urban basin to reach its peak discharge from dry condition. As flood monitoring pinpoints down to specific blocks, the temporal variability is even higher and a sampling at 5~6 minutes can miss the local peaks. For short-range radar, flexible waveforms and agile scan strategy can be adopted. In a dense radar network, scan patterns can be coordinated in an automatic and adaptive manner in response to the detected weather phenomena. For example, full volume scan can be performed when wide spread shallow storm is present; whereas narrower sector scan can be performed at multiple elevation angles to observe the vertical structure when deep convective storm happens.

2.3. Beam Height

Radar measurement and rainfall estimates will be closer to the ground if they are obtained at lower local heights. The radar beam also needs to be contained below bright bands or melting layers and above the significant mainlobe clutter to avoid QPE biases. The earth's curvature and the blockage by the local terrain can even prevent the coverage of raining regions of interest. The lowest beam height depends on radar range and the lowest available elevation angle. At long range, the beam height becomes extremely high because of the earth's curvature, e.g., nearly 5.3 km at 300 km range even at 0^o elevation angle. For good radar QPE, we prefer to have the lowest beam height to be kept around one km. For comparison, this can be achieved at 1^o elevation angle if the maximum range is limited to 50 km.

2.4. Sensitivity

The sensitivity of weather radar is proportionally related to the transmit power and inversely related to the square of radar range. Long duration light rain is not an apparent threat to an urban watershed because the drainage can discharge the runoff in time. When using gauge measurements to validate radar QPE, the gauge may not respond well to light rain either. For example, a tip bucket rain gauge of 0.01in per bucket will not tip in a single 5-minute interval for 2.5mm/hr rainfall, which is approximately translated to 30 dBZ for radar reflectivity or 0.1deg/km for the specific differential propagation phase. Especially, at X-band, an extra margin also needs to be allocated for the transmit power budget to compensate for the rain attenuation. Statistically rain attenuation is more likely to be higher at longer propagation path. Altogether, short range radar largely relaxes the constraint on sensitivity.

2.5. Clutter Mitigation

The radar reflectivity for clutter echo can be written as

$$Z_{ec} < dBZ >= 2f(\alpha) + \sigma^0 < dB > + C + 10\log_{10}\frac{A_c < km^2 >}{V_c < km^3 >} \quad (1)$$

where $f(\alpha)$ is the sidelobe pattern at clutter incidence angle, σ_0 is surface backscattering coefficient, C is the radar constant, A_c is the beam illuminated area, and V_c is the effective radar resolution volume. At low grazing angles, A_c is proportional to range. At low elevation angles and close ranges, ground based radar can suffer significant ground clutter contamination. Reflection from buildings can have a high grazing angle and in this case σ^0 can be larger by several orders. When these buildings intercept mainlobe, substantial beam lockage resulted. Use of the small-size radar enables flexible deployment if necessary such that mainlobe clutter can be avoided, for example, with rooftop installation on tall buildings, even though it can also increase the occurrence of sidelobe clutter.

3. X-BAND DUAL-POLARIZATION RADAR NETWORKS

A Distributed Collaborative Adaptive Sensing (DCAS) system dynamically utilizes networked short-range radar units to achieve high spatiotemporal resolution (McLaughlin et al. 2005). In DCAS networks, distributed short range radars are densely deployed among which the resources are dynamically and adaptively allocated according to the weather evolution and user needs, achieving higher resolution in both space and time. All the radar nodes are operated collaboratively to provide the sensing functionality for the entire network coverage. Overlapped radar coverage is systematically designed to provide rich information for later fusion and neighboring radars can be coordinated in real time to pinpoint the features of interest. As a dense deployment, a DCAS network consists of many radar nodes, demanding a cost-efficient development and installation of radar. As a result, the operation band is moved to short-wavelength, such as X-band.

3.1. CASA IP1

CASA has deployed a networked X-band radar test bed, named as Integrated Project 1 (IP1), in southwestern Oklahoma. The IP1 test bed is the first DCAS system of this kind developed and operated by CASA, primarily to monitor and respond to severe thunderstorms, heavy rainfall, and severe winds. The test bed covers a 7,000 km^2 region in southwestern Oklahoma that receives an average of 4 tornado warnings and 53 thunderstorm warnings per year, under the NEXRAD coverage of the KFDR and KTLX radars, as depicted in Fig.1.

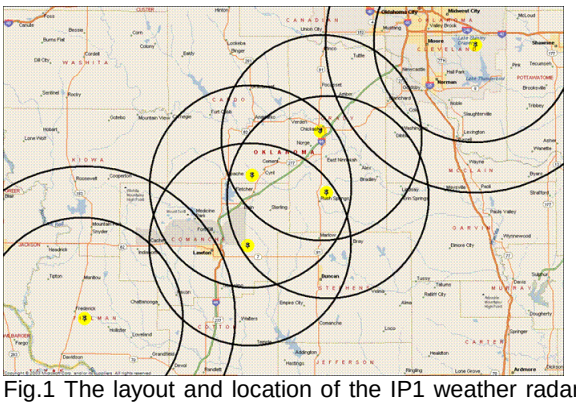

Fig.1 The layout and location of the IP1 weather radar network. The coverage circles of IP1 radar are in radius of 40km. KTLX is to the northeast of the test bed and KFDR is to the southwest of the test bed.

It is an end-to-end system of a network of four, low-power, short-range, dual polarization, Doppler radar units. Each radar is operated with a maximum range of 40km and a maximum elevation angle of 30^o. The four radar nodes are located in the towns of Chickasha (KSAO), Rush Springs (KRSP), Cyril (KCYR) and Lawton (KLWE), OK, and each radar node is approximately 30 km away from the next unit. Connected to Internet, these four IP1 radars transfer real-time observations to a server known as System Operations Control Center (SOCC), located in the National Weather Center building in Norman, OK, where radar data are fused and processed. A Meteorological Command and Control (MC&C) system is also installed in SOCC which detects the weather features such as storm cells and circulations, optimizes resource allocation according to end-user's needs, and generate new scan tasks to reconfigure all the radar nodes (Zink et al. 2008). The system update time can be as fast as 1 minute due to the implementation of adaptive, coordinated sector scanning strategy.

3.2. NIED X-NET

The National Research Institute for Earth Science and Disaster Prevention (NIED), Japan is in the

process of establishing an urban radar network (X-NET) in Tokyo-to (Metropolitan Tokyo) (Maki et al. 2008), as shown in Fig.2. The Tokyo metropolitan area is the world's most populous metropolitan area, where about 30 million people lives within 50km radius, including 5 mega cities. The network consists of 3 X-band dual-polarization radars, whose coverage is delineated in red circles as shown in Fig.2. Each radar has a beamwidth about 1.3^o and a maximum range of 80 km, and can be re-configured for sector scan, volume scan and RHI scan. Two additional research radars and 2 operational radars are planned to be networked in 2010.

One of the primary goals of X-NET is to develop operational warning systems for disasters arising from heavy rainfall. Urban flood prediction and landslide disaster prediction are the most important applications under development using the achieved quantitative rainfall estimates. The real-time flood-risk mapping system employs flood risk data at 10 m resolution and a 1-hour lead time.

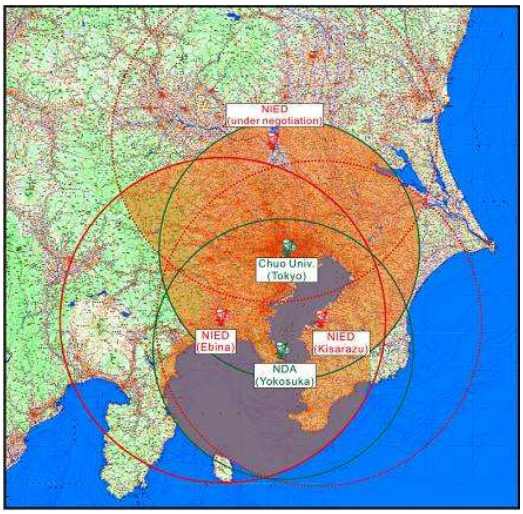

Fig.2 Location and radar sites of the X-NET test bed in metropolitan Tokyo. The coverage of three dual-polarization radars is marked in red line of 80 km radius.

4. DUAL POLARIZATION QUANTITATIVE PRECIPITATION ESTIMATION

Derivation of quantitative rainfall estimates from radar observations is known as a highly challenging process because of the inherent variability of hydrometeorological processes. The microphysical variability can be largely accounted for using dual polarization measurements, such as combinations of the radar reflectivity, the differential reflectivity, and the specific differential propagation phase (Bringi and Chandrasekar 2001). Rainfall estimation from K_{dp} is particularly appealing in X-band radar networks, because 1) it avoids the uncertainty in attenuation correction; 2) K_{dp} is sensitivity to light rainfall at short wavelengths; 3) it does not need network calibration for the four radar nodes.

Fundamentally radar QPE is built upon physical models of the rain medium relating between rain microphysics and radar observables (Bringi and Chandrasekar 2001). The R-K_{dp} relation can be expressed in a power law form as,

$$R = aK_{dp}^{b} \qquad (2)$$

Due to the frequency scaling, K_{dp} responds well to low rainfall rate at X-band (compared to S-band) such that R-K_{dp} conversion can be directly applied in light rain circumstance; on the other hand, K_{dp} can also exhibit a steeper slope within an intensive rain cell. The estimation of K_{dp} is a challenge as the range derivative of the differential propagation phase profiles. It subjects to substantial fluctuations, especially at low rain rates, that need to be suppressed with a strong filter. However, the filter will smooth out the peaks on the other hand and hence introduce biases at high rain rates (Gorgucci 1999). An adaptive K_{dp} algorithm automatically tuned to the spatial gradient of K_{dp} was implemented in the CASA IP1 testbed that substantially reduces the fluctuation in light rain and the bias at heavy rain (Wang and Chandrasekar 2009). Fig.3(a) shows a snapshot of K_{dp} estimates for each IP1 radar. It can be seen that the K_{dp} field is fairly stable in the low rain rate regions and is fairly high in the storm cores.

The IP1 testbed was designed with overlapping coverage among its radar nodes. The independence of K_{dp} on the radar calibration enables flexibility in combining the collocated K_{dp} estimates from all the radar nodes. It is the K_{dp} field, rather than the rainfall field, to be merged because we want to further reduce the variation on the input to the nonlinear R-K_{dp} conversion. The composite K_{dp} field comes from the radar with lowest beam height and nearest slant range, or from the radar with the best K_{dp} estimates. Moreover, the data availability is further enhanced by the overlapped topology in cases of heavy rainfall, or blockage or any other factor requiring redundancy demonstrating the operational strength of the network centric system.

In the IP1's DCAS scan strategy, the 2^o scan is a surveillance scan, interleaved into a set of optimized scans from 1^o up to 30^o. To drive the rainfall conversion, only K_{dp} from the 2^o scan is used. The 2^o scan is also a good choice for QPE because the beam width of IP1 radars is about 2^o. At 2^o elevation angle, the clutter would come from sidelobes and its impact would be minimal after clutter filtering. In X-NET, the lowest two PPI sweeps (at 2.1^o and 4.4^o) are used to form a composite scan for better coverage of the mountainous regions. Fig.3(a) shows the estimated K_{dp} field for each IP1 radar within the system "heartbeat" of update time. The storm was passing over the center of network coverage and each radar node has full or partial view of the storm. Fig.3(b) displays the merged K_{dp} field of Fig.3(a) based on the nearest range, which is also the lowest beam height because of the fixed elevation angle. Fig.3(c) displays the merged field based on the data quality of the differential phase. Visually there is little difference between these two methods shown here. Both create a complete coverage of the storm, much better than individual radar does. However, critically evaluating a large number of data sets, it has been seen that the second procedure is better.

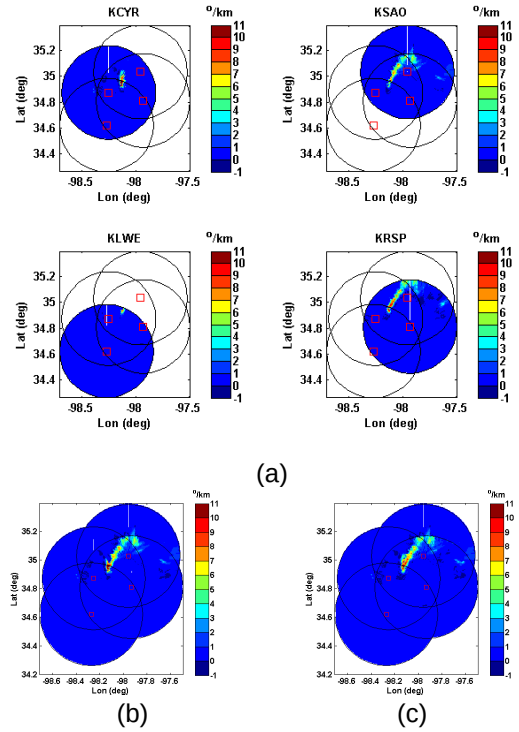

Fig.3 Composite K_{dp} estimates from the IP1 radar network, on 08:12 UTC, May 27, 2008.

5. IMPLEMENTATION AND SYSTEM ARCHITECTURE

With the common goal to providing real-time urban floods monitoring, CASA and NIED have established a partnership. The IP1 network and X-NET are developed with similar technologies, yet have distinct operational configurations and characteristics. The IP1 network is operated over a set of dynamic scan strategies where new scan protocols are continuously developed and evaluated with a diverse end-user base. The network centric sensing can be investigated at full scales. X-NET is operated with a fairly stable scan strategy. Tokyo, one of the most populous and densest metropolises, experiences a humid subtropical climate with occurrence of typhoons and summer thunderstorms. The interaction between radar rainfall estimation and hydrological model will be one of the core parts of the X-NET testbed, to provide the local residents advanced flood warnings at various urbanized locations. A system diagram for this application is described in Fig.4, where the high-resolution hydrologic model is eventually integrated into a DCAS network. As an end-to-end system, multiple aspects of disaster prevention will be investigated, including data fusion, rainfall estimation, short-term precipitation forecast, and user impact. The interaction between flood warnings and people response will also be investigated, in order to deliver better risk information to the residents of different social and cultural requirements.

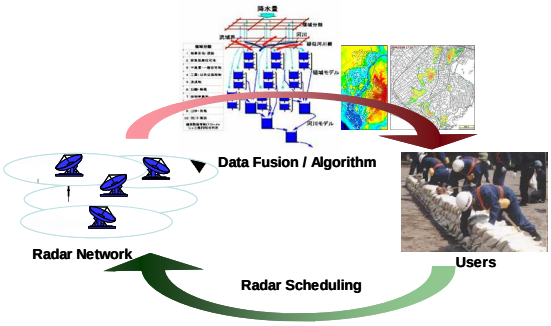

Fig.4 System diagram of urban floods monitoring system integrated into a DCAS radar network.

The experience producing real time products and the initial validation work done at both NIED and CASA will be very useful in launching the urban flood forecast network in this test bed. Both CASA and NIED had conducted preliminary and encouraging early validation studies on radar rainfall estimation using X-band dual-polarization radar. The metrics of validation include the mean

bias, the normalized mean bias and the normalized standard error, defined respectively as follows:

$$< e >= \langle R_R - R_G \rangle \quad (3)$$

$$< e >_N = \frac{\langle R_R - R_G \rangle}{\langle R_G \rangle} \quad (4)$$

$$NSE = \frac{\langle |R_R - R_G| \rangle}{\langle R_G \rangle} \quad (5)$$

where brackets denote sample average, R_R is the radar estimate and R_G is the gauge measurement of instantaneous rainfall rate or hourly rainfall accumulation.

Since 2007, several intensive operation experiments had been conducted in IP1, mostly during the spring storm season, to demonstrate and evaluate the fundamental concept of DCAS system and investigate the value added impact of this networked weather radar system compared to conventional weather radar systems (Chandrasekar et al. 2008). A wide range of coefficients has been reported for the R-K_{dp} power law relation at both S-band and X-band. For fair comparison, the KOUN's R-K_{dp} relations was selected, that has been evaluated at S-band for the prototype WSR-88D system (Ryzhkov et al. 2005). The relation was scaled to X-band with respect to wavelength for rainfall conversion in the IP1 test bed, resulted as

$$R = 18.15 K_{dp}^{0.791} \quad (6)$$

The performance of the IP1 QPE product was evaluated for all major rain events against the USDA Agriculture Research Service's gauge network (MicroNet) in the Little Washita watershed, which comprises 20 weather stations in the center of the test bed as shown in Fig.5.

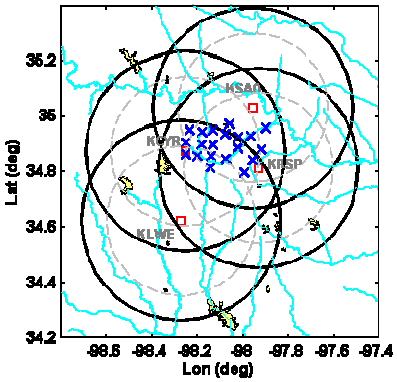

Fig. 5 Location of the USDA ground gauges in the CASA's IP1 network.

In total, 29 storm events from the CASA experiments are analyzed in this paper, including events of different storm types such as severe thunderstorm, convective line, wide spread stratiform rain, and cold front system. Overall the hourly rainfall estimates compared to the gauge measurements have a very small bias of 4.26% and a normalized standard error of 22.76%. Event wise, the hourly rainfall estimates have a bias less than 10% and a NSE less than 30% for most of the events.

Similarly, ground validation with gauges and disdrometers was performed in X-NET. Four of the gauges were installed along a line in the mountainous area with 10km spacing and another four gauges were installed 10km away from the radar node as shown in Fig.6. The rainfall rate was computed using a composite algorithm as

$$R = \begin{cases} 19.6 K_{dp}^{0.823} & K_{dp} > 0.3^o / km \\ 7.07 \times 10^{-3} Z_h^{0.819} & K_{dp} \le 0.3^o / km \end{cases} \quad (7)$$

which was derived from scattering simulation. Observations from three long duration precipitation events, including two straitform and one typhoon case, were used to test the rainfall estimation algorithm using the X-band radar. It delivered excellent rainfall estimates with a normalized bias of 1.1% and a normalized error of 14.8% in hourly rainfall accumulation (Park et al 2005).

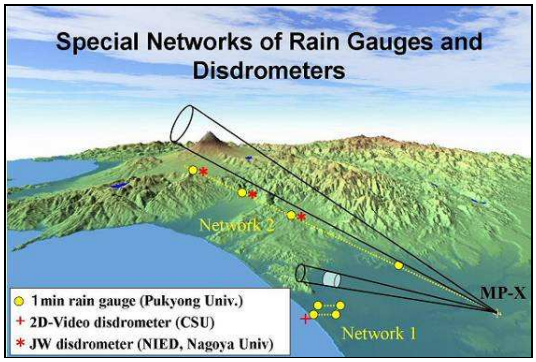

Fig.6 One of the X-NET radar nodes and the set up of ground gauge network.

6. SUMMARY

This paper presents the process and performance of high-resolution quantitative precipitation estimation (QPE) in an X-band dual-polarization radar network, which will potentially improve floods warning. High spatiotemporal resolution is also one of the essential requirements for predication and prevention of flash floods and

urban floods. Urban development reduces the response time of urban watersheds to rainfall and increases the peak discharge volumes. Incorporated with high-resolution rainfall mapping, physically based distributed hydrologic models have critical advantage for accurate monitoring of urban watersheds and drainage networks.

A DCAS network of short-range radar can observe the weather with high resolution and low beam height. The current temporal resolution in CASA is 60 seconds, which can be improved to 30 seconds for rainfall mapping. The spatial resolution is variable with a median value of about 300 m in the common area of the IP1 test bed. Its performance was demonstrated using networked radar rainfall mapping algorithm through ground validation. The fundamental limitation of long range radar, such as beam broadening and earth curvature blockage, is overcome by the dense deployment of a DCAS radar network. Accordingly, high resolution observations can be achieved with small-size radar units throughout the network coverage using coordinated, collaborative scanning. From a practical viewpoint, preparing the infrastructure to support the conventional long-range radar system is an overwhelming task in urban environment, due to the social footprint of such systems. This in fact is part of the motivation driving the deployment of small-size X-band radars.

The multi-year validation studies have shown encouraging match between radar QPE and ground measurements. It demonstrates the operational feasibility using X-band dual-polarization radar for accurate rainfall mapping and, in combination with the high resolution, further for driving the urban floods warning systems. A partnership has been established between CASA and NIED to promote the development and operation of such end-to-end networked system. Within the next two years, Japan decided to deploy four operational networked radar systems for flood mitigation in four metropolitan areas namely, Tokyo, Kyoto, Osaka and Kanazawa, led by Ministry of Land, Infrastructure, Transport and Tourism. In total about 70 million people live in these four industrial centers where the successful deployment of the radar networks will have important social impact and economic values.

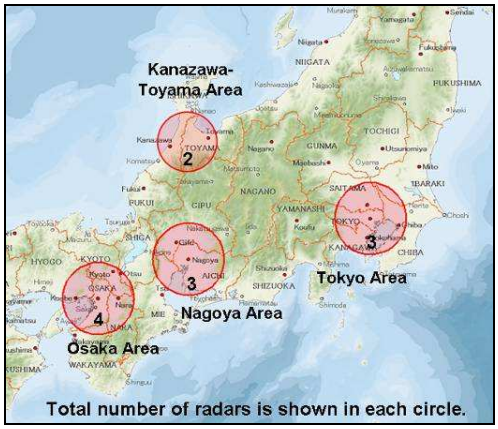

Fig.7 The planed X-band dual-polarization radar networks in Japan for rainfall estimation and urban floods mitigation.

Acknowledgement This research is supported by the National Science Foundation via the NSF/Engineering Research Center Program ERC-0313747, and by the National Research Institute for Earth Science and Disaster Prevention (NIED), Japan.

References

Bringi, V.N. and V. Chandrasekar, 2001: Polarimetric Doppler Weather Radar: Principles and applications. Cambridge University Press. 648 pp.

Chandrasekar, V., D.J. McLaughlin, J. Brotzge, M. Zink, B. Philips, and Y. Wang, 2008: Distributed Collaborative Adaptive Radar Network: Preliminary Results from the CASA IP1 Testbed, Preprint, 2008 IEEE Radar Conference, Rome, Italy.

Gorgucci, E., G. Scarchilli, and V. Chandrasekar, 1999: Specific Differential Phase Estimation in the Presence of Nonuniform Rainfall Medium along the Path. J. Atmos. Oceanic Technol., 16, 1690–1697.

Junyent F, and Chandrasekar V, 2008: Theory and characterization of weather radar networks. Journal of Atmospheric and Oceanic Technology: in press.

Maki, M, T. Maesaka, R. Misumi, K. Iwanami, S. Suzuki, A. Kato, S. Shimizu, K. Kieda, T. Yamada, H. Hirano, F. Kobayashi, A. Masuda, T. Moriya, Y. Suzuki, A. Takahori, D. Lee, D. Kim, V. Chandrasekar, Y. Wang, 2008: X-band Polarimetric Radar Network in the Tokyo Metropolitan Area – X-NET, The fifth European Conf. Radar Meteor. Hydrology, Helsinki, Finland.

McLaughlin, D.J., V. Chandrasekar, K. Droegemeier, S. Frasier, J. Kurose, F. Junyent, B. Philips, S. Cruz-Pol, and J. Colom, 2005: Distributed Collaborative Adaptive Sensing (DCAS) for Improved Detection, Understanding, and Prediction of Atmospheric

Hazards, 9th Symp. Integrated Obs. Assim. Systems, Amer. Meteor. Soc..

National Research Council, 2005: Flash Flood Forecasting Over Complex Terrain: With an Assessment of the Sulphur Mountain NEXRAD in Southern California. National Academy Press.

National Research Council, 2008: Observing Weather and Climate from the Ground Up: A Nationwide Network of Networks. National Academy Press.

Park, S.G., M. Maki, K. Iwanami, V.N. Bringi, and V. Chandrasekar, 2005: Correction of Radar Reflectivity and Differential Reflectivity for Rain Attenuation at X Band. Part II: Evaluation and Application. J. Atmos. Oceanic Technol., 22, 1633–1655.

Ryzhkov, A.V., S.E. Giangrande, and T.J. Schuur, 2005: Rainfall Estimation with a Polarimetric Prototype of WSR-88D. J. Appl. Meteor., 44, 502–515.

Ryzhkov, A.V., 2007: The Impact of Beam Broadening on the Quality of Radar Polarimetric Data. J. Atmos. Oceanic Technol., 24, 729-744.

Vieux, B.E., and P.B. Bedient, 2004: Assessing urban hydrologic prediction accuracy through event reconstruction. J. Hydrology, 299, 217-236.

Zink M., E. Lyons, D. Westbrook, J. Kurose, and D. Pepyne, 2008: Closed-loop Architecture for Distributed Collaborative Adaptive Sensing of the Atmosphere: Meteorological Command & Control, International J. Sensor Networks, InderScience, in press.

Wang Y, and V. Chandrasekar, 2009: Algorithm for Estimation of the Specific Differential Phase. J. Atmos. Oceanic Technol., In Press.